Spin-valley coupling in the strongly correlated limit of twisted bilayer BC_3

Toshikaze Kariyado

MANA, NIMS

28 Nov 2022

Acknowledgment: A. Vishwanath

arXiv:2206.14835

Outline

- Introduction
  - Quick overview of twisted bilayer systems
  - Quantum interfernce, interlayer tunneling, and valleys
- Twisted Bilayer BC_3
  - Monolayer band structure
  - Twisted bilayer band structure
  - Strongly correlated limit – Hubbard model
  - Strongly correlated limit – spin-valley model

Background

mismatched stacking → moiré pattern → effective potential → band structure manipulation

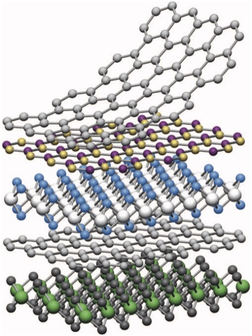

Geim & Grigorieva, Nature **499**, 419 (2013).

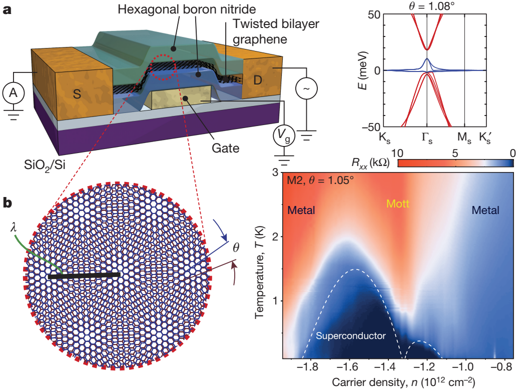

Cao *et al.*, Nature **556**, 43/80 (2018).

Quick Review of Moiré Bilayers

$$H = \begin{pmatrix} H_0^+(-i\vec{\nabla}) & V(\vec{r}) \\ V^\dagger(\vec{r}) & H_0^-(-i\vec{\nabla}) \end{pmatrix}$$

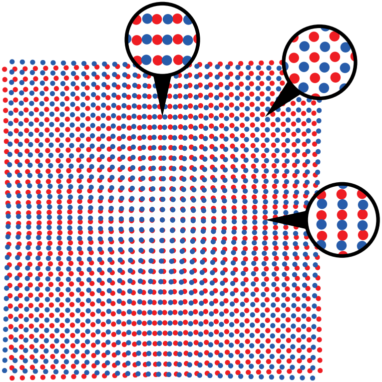

- parabolic

$$H_0(-i\vec{\nabla}) = -\frac{\hbar^2}{2m}\vec{\nabla}\cdot\vec{\nabla}$$

- Dirac

$$H_0(-i\vec{\nabla}) = v(-i\vec{\nabla})\cdot\vec{\sigma}$$

position dependent tunneling $V(\vec{r})$

Quick Review of Moiré Bilayers

$$H = \begin{pmatrix} H_0^+(-i\vec{\nabla}) & V(\vec{r}) \\ V^\dagger(\vec{r}) & H_0^-(-i\vec{\nabla}) \end{pmatrix}$$

Basis transformation

$$H' = \begin{pmatrix} \tilde{H}(-i\vec{\nabla}) + |V(\vec{r})| & 0 \\ 0 & \tilde{H}(-i\vec{\nabla}) - |V(\vec{r})| \end{pmatrix} + O(H_0^+ - H_0^-)$$

$$\tilde{H}(-i\vec{\nabla}) = H_0^+(-i\vec{\nabla}) + H_0^-(-i\vec{\nabla} + \vec{\nabla}\varphi(\vec{r})), \quad V(\vec{r}) = e^{i\varphi(\vec{r})}|V(\vec{r})|$$

$|V(\vec{r})|$ works as effective potential!

Quick Review of Moiré Bilayers

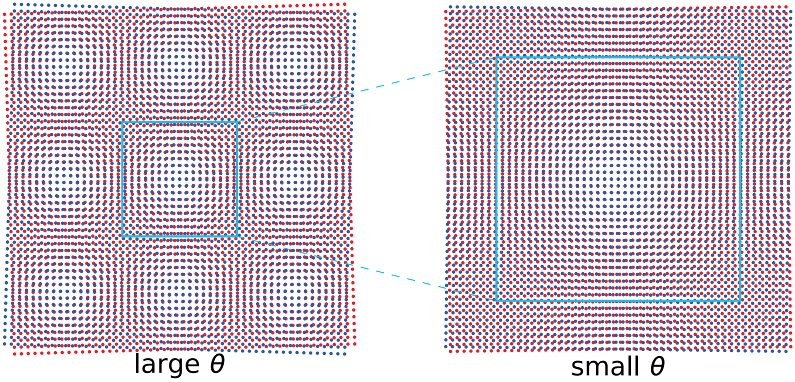

Quick Review of Moiré Bilayers

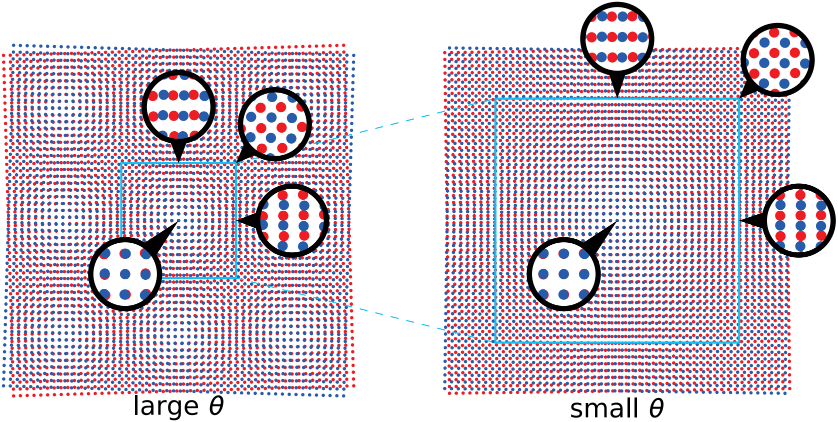

$$V(\vec{r})|_{\theta=\theta_1} \sim V(\alpha\vec{r})|_{\theta=\theta_2}, \quad \alpha = \frac{L(\theta_2)}{L(\theta_1)}$$

Moiré Bilayer: Theoretical Minimum

Scale transformation $\vec{r} \to \alpha\vec{r}$

$$\tilde{H} = \begin{pmatrix} \tilde{H}_0^+(-i\alpha^{-1}\vec{\nabla}) & \tilde{V}(\alpha\vec{r}) \\ \tilde{V}^\dagger(\alpha\vec{r}) & \tilde{H}_0^-(-i\alpha^{-1}\vec{\nabla}) \end{pmatrix}$$

- parabolic

$$\tilde{H} = \begin{pmatrix} \alpha^{-2}H_0^+(-i\vec{\nabla}) & V(\vec{r}) \\ V^\dagger(\vec{r}) & \alpha^{-2}H_0^-(-i\vec{\nabla}) \end{pmatrix} = \frac{1}{\alpha^2}\begin{pmatrix} H_0^+(-i\vec{\nabla}) & \alpha^2 V(\vec{r}) \\ \alpha^2 V^\dagger(\vec{r}) & H_0^-(-i\vec{\nabla}) \end{pmatrix}$$

- Dirac

$$\tilde{H} = \begin{pmatrix} \alpha^{-1}H_0^+(-i\vec{\nabla}) & V(\vec{r}) \\ V^\dagger(\vec{r}) & \alpha^{-1}H_0^-(-i\vec{\nabla}) \end{pmatrix} = \alpha^{-1}\begin{pmatrix} H_0^+(-i\vec{\nabla}) & \alpha V(\vec{r}) \\ \alpha V^\dagger(\vec{r}) & H_0^-(-i\vec{\nabla}) \end{pmatrix}$$

moiré length $\longleftrightarrow$ balance between kinetic & potential energy

Quantum Interference and Effective Tunneling

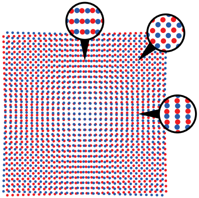

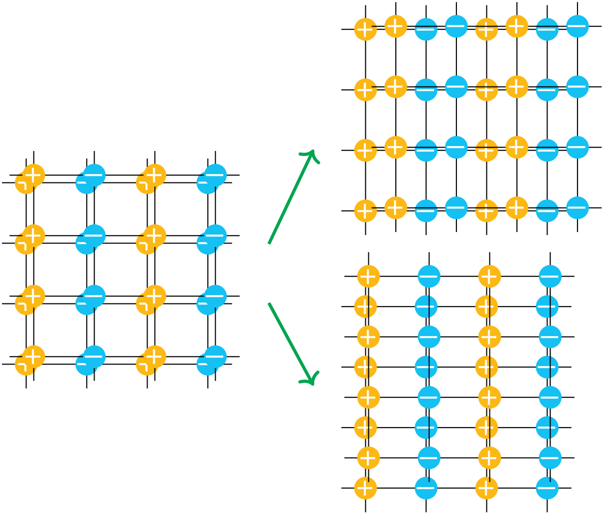

Interference of Bloch wave functions has a striking effect on the interlayer tunneling!

Valley Physics

phase pattern ↔ in-plane momentum ↔ valley dependence

$$\psi(\vec{r}) = e^{i\vec{k}\cdot\vec{r}} u_{\vec{k}}(\vec{r})$$

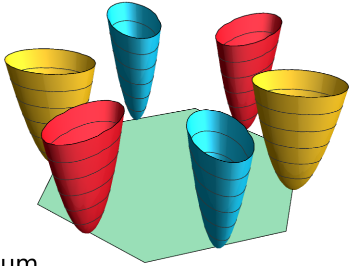

Each valley has its own representative momentum.

Outline

- Introduction
  - Quick overview of twisted bilayer systems
  - Quantum interfernce, interlayer tunneling, and valleys
- Twisted Bilayer BC_3
  - Monolayer band structure
  - Twisted bilayer band structure
  - Strongly correlated limit – Hubbard model
  - Strongly correlated limit – spin-valley model

Monolayer BC_3

exp. fabrication: Tanaka *et al.*, Solid State Commun. **136**, 22 (2005).

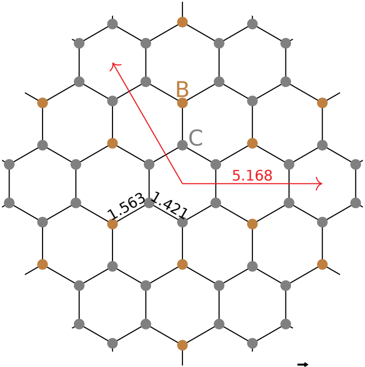

QuantumEspresso
crystal str.: rev-vdW-DF2
electronic str.: PBE-GGA

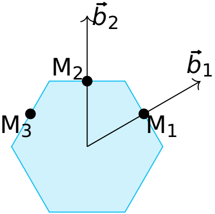

3 valleys!

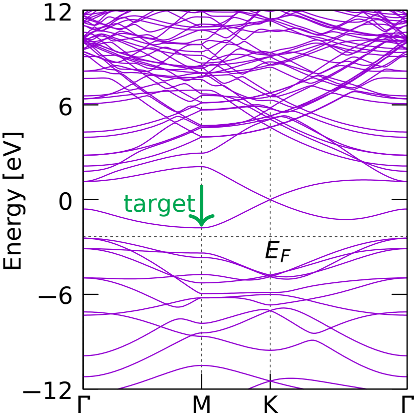

Monolayer BC_3

exp. fabrication: Tanaka *et al.*, Solid State Commun. **136**, 22 (2005).

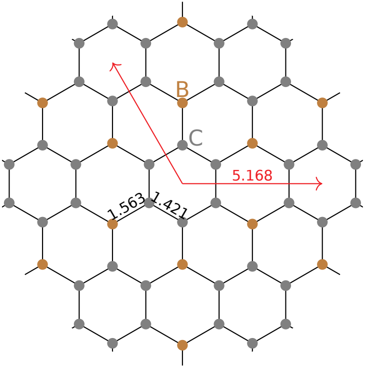

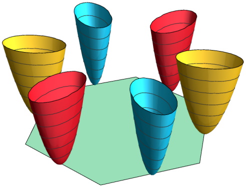

QuantumEspresso
crystal str.: rev-vdW-DF2
electronic str.: PBE-GGA

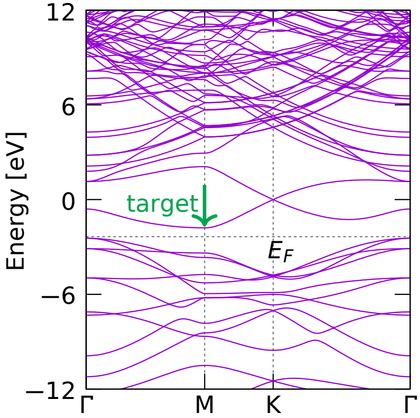

Wave Functions

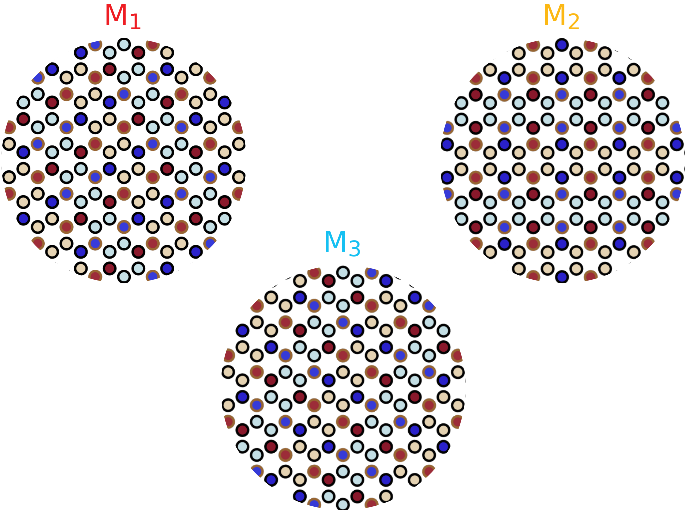

Effective Tunneling

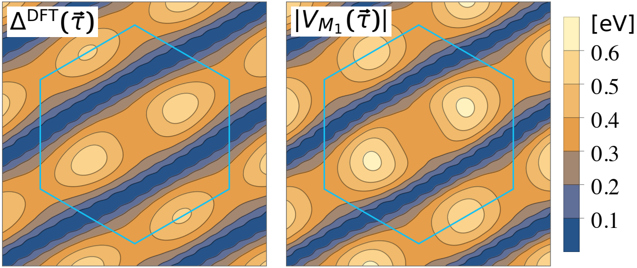

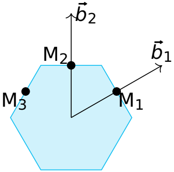

Interlayer Tunneling from Tight-Binding Model

$$V_{\vec{k}}(\vec{\tau}) = e^{-i\vec{k}\cdot\vec{\tau}} \iint d\vec{r} d\vec{r}' \psi^*_{\vec{k}}(\vec{r}+\vec{\tau}) t_{\text{inter}}(\vec{r}-\vec{r}') \psi_{\vec{k}}(\vec{r}')$$

$$t_{\text{inter}}(\vec{r}) = v_0 \exp\Big(-\frac{2d_0(r_z - d_0)}{r_0^2}\Big) \exp\Big(-\frac{r_x^2 + r_y^2}{r_0^2}\Big), \quad d_0 = d_z(\vec{0})$$

$$v_0 = 0.30\text{eV},\ r_0 = 2.0\text{Å}$$

Twisted Bilayer BC_3

valley superposed

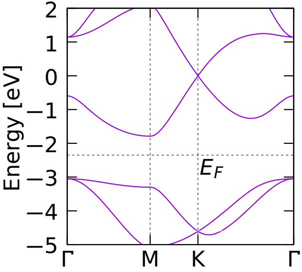

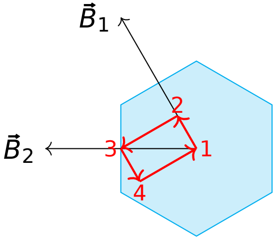

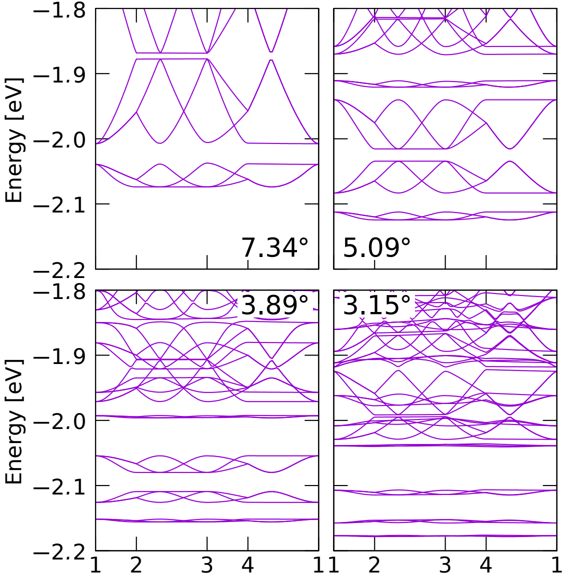

Twisted Bilayer BC_3

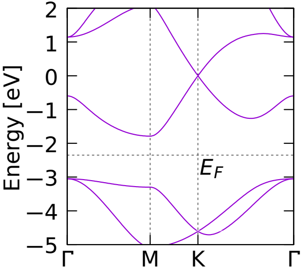

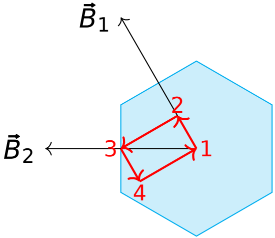

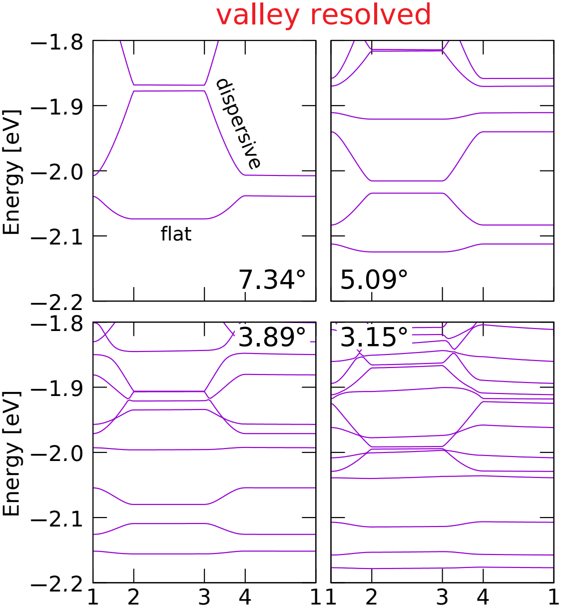

“Big” Wannier functions

bilayer $\vec{k}\cdot\vec{p}$ model → one Wannier orbital per a “big” moire cell

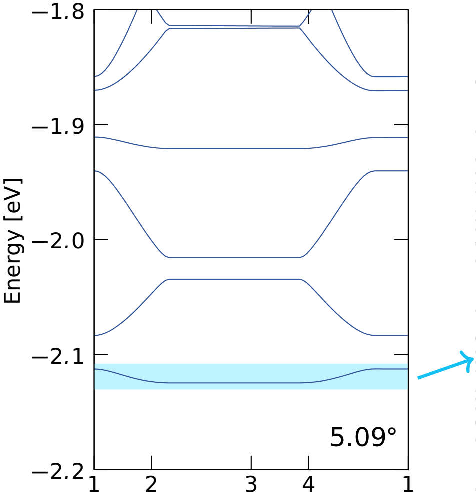

color: $|w_{\mathrm{upper}}(\vec{r})|^2+|w_{\mathrm{lower}}(\vec{r})|^2$

lines: contour of $|V_{\vec{k}}(\vec{\tau}(\vec{r}))|$

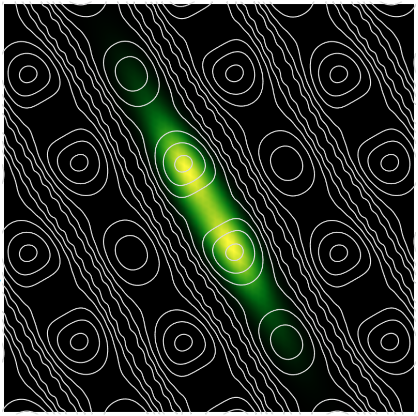

Three Valleys

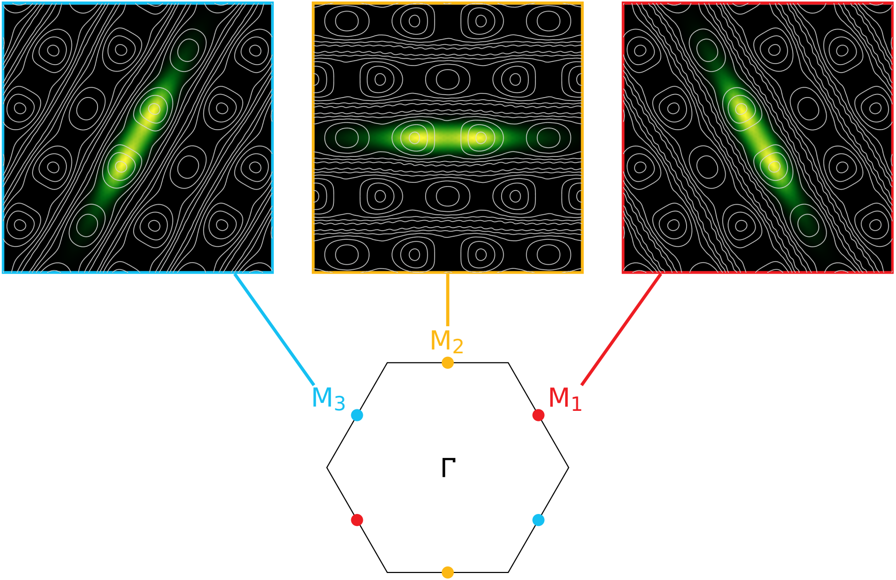

Effective Tight-Binding Model

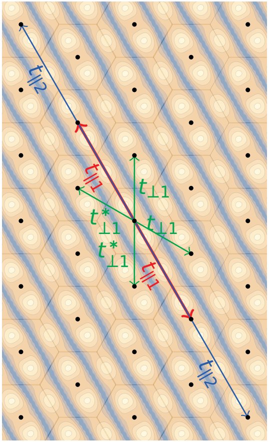

color: $|V_{\vec{k}}(\vec{\tau}(\vec{r}))|$

$\{t_{\parallel 1}, t_{\parallel 2}, t_{\parallel 3}, t_{\parallel 4}, t_{\perp 1}\}$-model

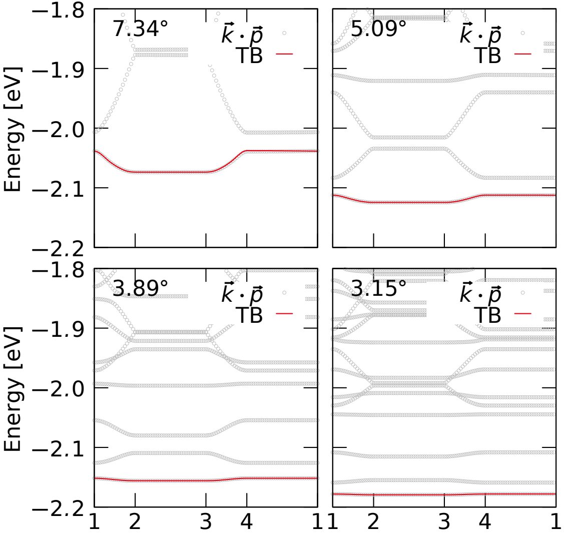

Effective Tight-Binding Model

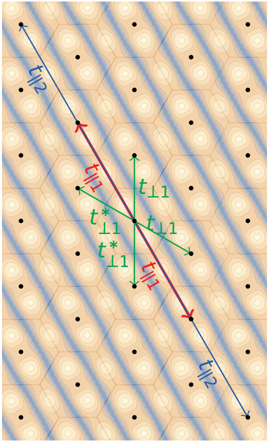

color: $|V_{\vec{k}}(\vec{\tau}(\vec{r}))|$

$\{t_{\parallel 1}, t_{\parallel 2}, t_{\parallel 3}, t_{\parallel 4}, t_{\perp 1}\}$-model

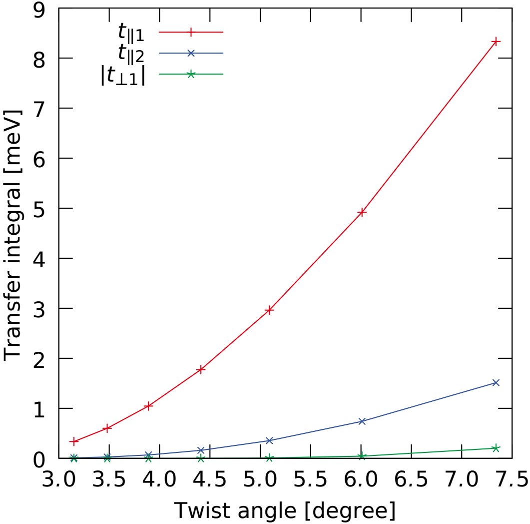

$t_{\parallel 1}$ only model

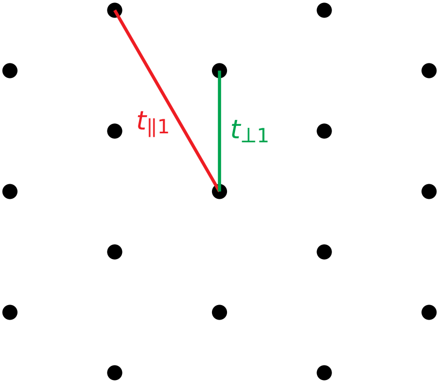

$t_{\parallel 1}$ only model

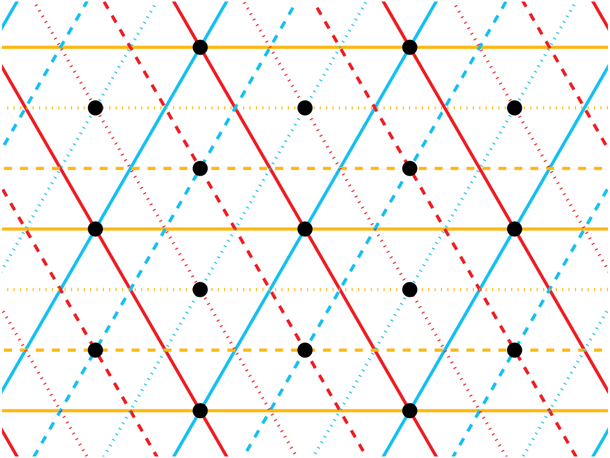

nested network of three *decoupled* triangular lattices

$t_{\parallel 1}$ only model

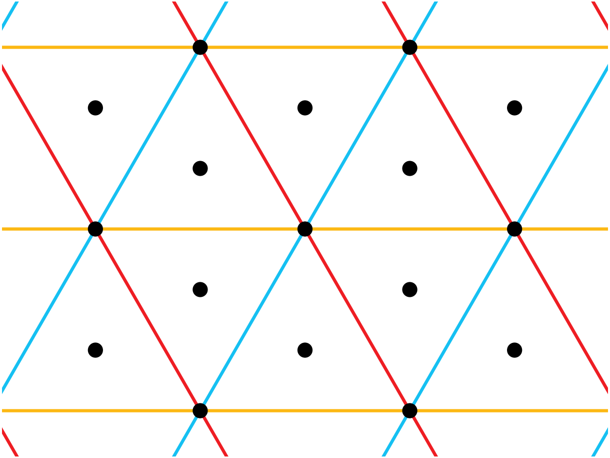

nested network of three *decoupled* triangular lattices

Three Orbital (Three Valley) Hubbard Model

$$H = t_{\parallel 1} \sum_{\vec{r}\sigma} \sum_{\mu=1}^{3} c^{\dagger}_{\vec{r}+\vec{e}_\mu,\mu\sigma} c_{\vec{r},\mu\sigma} + \text{ h.c.}$$

$$+ U \sum_{\vec{r}} \sum_{\mu=1}^{3} n_{\vec{r},\mu\uparrow} n_{\vec{r},\mu\downarrow} + U' \sum_{\vec{r},\sigma\sigma'} \sum_{\mu<\mu'} n_{\vec{r},\mu\sigma} n_{\vec{r},\mu'\sigma'}$$

- U, U': intra- and inter-orbital onsite repulsion
- Hund and pair hopping terms: neglected

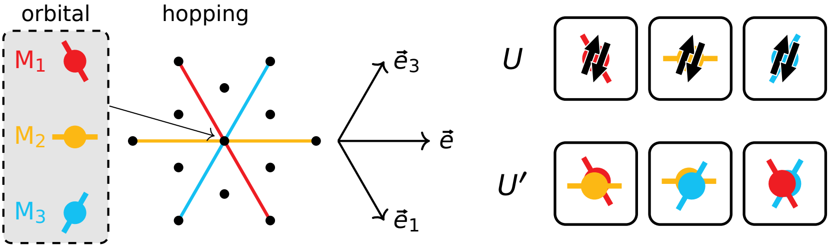

Strongly Correlated Limit – BC_3

Orbital (valley) dependent superexchange!

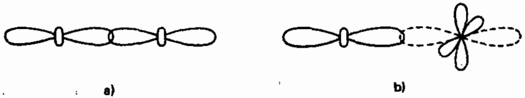

FIG. 11. Various possible types of overlay of e_g orbitals at neighboring centers. a—the overlap of single filled orbitals, which leads to a strong antiferromagnetic exchange interaction; b—the overlap of filled orbitals is zero. A filled orbital and an empty orbital (dashed line) overlap, and the exchange is accordingly ferromagnetic.

Kugel & Khomskii, Soviet Physics Uspekhi **25**, 231 (1982).

Spin-Orbital Model

$t \ll U, U'$ at one electron per moire unit (1/6 filling)

- local basis: $|\sigma\rangle \otimes |\tau\rangle$ ($\sigma =\uparrow,\downarrow$, $\tau =$M$_1$,M$_2$,M$_3$)

$$H_{\text{eff}} = J \sum_{\vec{r}} \sum_{\mu=1}^{3} \Big(\vec{S}(\vec{r}+\vec{e}_\mu) \cdot \vec{S}(\vec{r}) - \frac{1}{4} \Big) \tilde{\tau}_\mu(\vec{r}+\vec{e}_\mu) \tilde{\tau}_\mu(\vec{r})$$

$$- V \sum_{\vec{r}} \sum_{\mu \neq \mu'} \Big(\tilde{\tau}_{\mu'}(\vec{r}+\vec{e}_\mu) \tilde{\tau}_\mu(\vec{r}) + \tilde{\tau}_{\mu'}(\vec{r}-\vec{e}_\mu) \tilde{\tau}_\mu(\vec{r}) \Big)$$

$$J = \frac{4t^2}{U}, \quad V = \frac{t^2}{U'}, \quad (\tilde{\tau}_l)_{ij} = \delta_{il}\delta_{ij}$$

- variant of Kugel-Khomskii model
- orbital degrees of freedom: classical and frozen

Eigenstate (1)

Ferro-orbital order - **FOO**

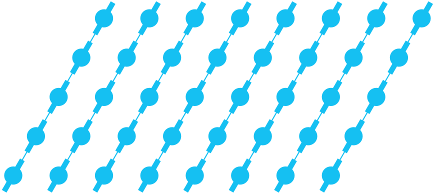

- decoupled spin-1/2 chains

$$E_{\text{per site}} = (-0.4431 - 0.25)J$$
$$\sim -2.8\frac{t^2}{U}$$

Eigenstate (2)

Fully antiferro-orbital order - **FAOO**

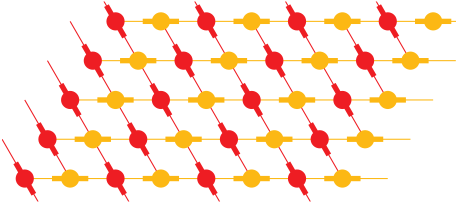

- $(-V) \times 2$ per site

$$E_{\text{per site}} = -2V = -\frac{2t^2}{U'}$$

Eigenstate (2)

Fully antiferro-orbital order - **FAOO**

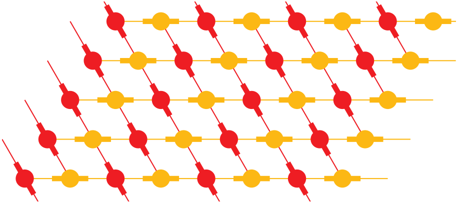

- $(-V) \times 2$ per site

$$E_{\text{per site}} = -2V = -\frac{2t^2}{U'}$$

Macroscopic number of degeneracy!

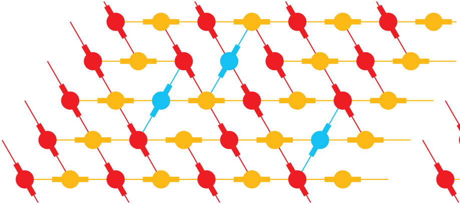

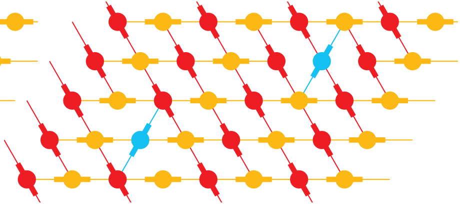

Eigenstate (3)

Dimer covering - **DC**

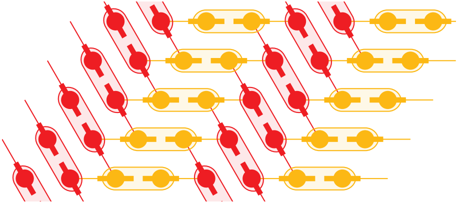

- $-J$ per singlet
- $(-V) \times 2$ per dimer

$$E_{\text{per site}} = -\frac{J}{2} - V = -\frac{2t^2}{U} - \frac{t^2}{U'}$$

Eigenstate (3)

Dimer covering - **DC**

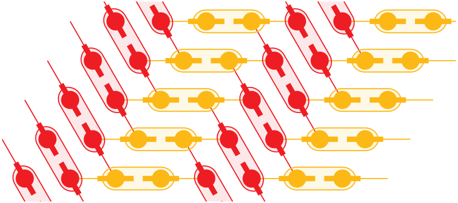

- $-J$ per singlet
- $(-V) \times 2$ per dimer

$$E_{\text{per site}} = -\frac{J}{2} - V = -\frac{2t^2}{U} - \frac{t^2}{U'}$$

Macroscopic number of degeneracy!

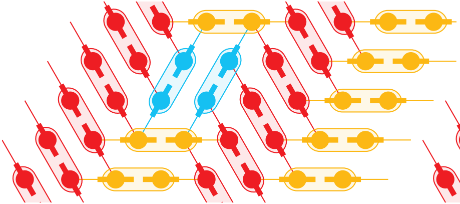

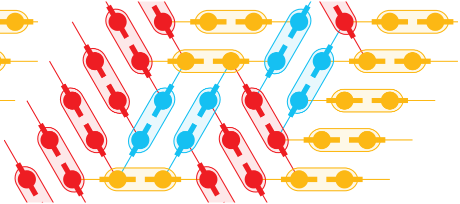

“Phase Diagram”

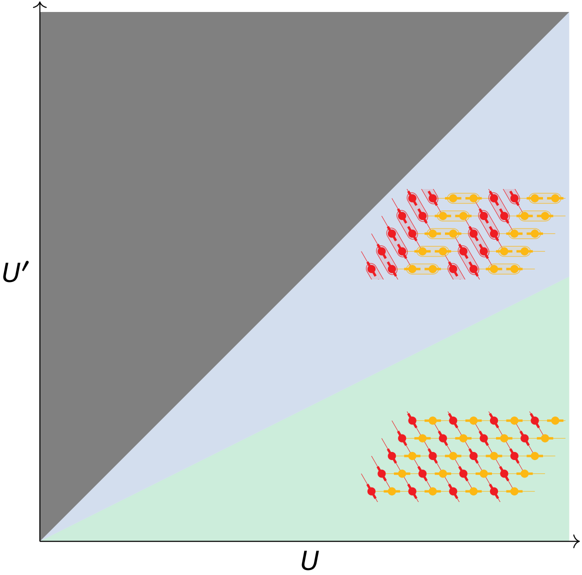

Rough Estimation of U and U'

$$U = v_{\alpha\alpha}, \quad U' = v_{\alpha\alpha'} \, (\alpha \neq \alpha')$$

$$v_{\alpha\alpha'} = \int d^2\vec{r} \int d^2\vec{r}' \rho_\alpha(\vec{r}) V(\vec{r} - \vec{r}') \rho_{\alpha'}(\vec{r}') = \frac{1}{(2\pi)^2} \int d^2\vec{q} \rho_{\alpha,\vec{q}} V_{\vec{q}} \rho_{\alpha',-\vec{q}}$$

$$f_{\vec{q}} = \int d^2\vec{r} e^{-i\vec{q}\cdot\vec{r}} f(\vec{r})$$

$$\rho_\alpha(\vec{r}) = |w^{(\alpha)}_{\text{upper}}(\vec{r})|^2 + |w^{(\alpha)}_{\text{lower}}(\vec{r})|^2$$

- bare Coulomb interaction

$$V_{\vec{q}} = \frac{2\pi k_0 e^2}{\bar{\epsilon} q}, \quad k_0 = \frac{1}{4\pi\epsilon_0}, \quad \bar{\epsilon} = \frac{\epsilon}{\epsilon_0}$$

- screening by metallic gates at $z = \pm d_{\text{gate}}$

$$V_{\vec{q}} = \frac{2\pi k_0 e^2}{\bar{\epsilon} q} \tanh(q d_{\text{gate}})$$

U vs U' vs W

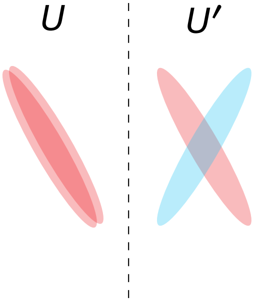

- $W = 4t_{\parallel 1}$
- $U > 2U'$ at small angle

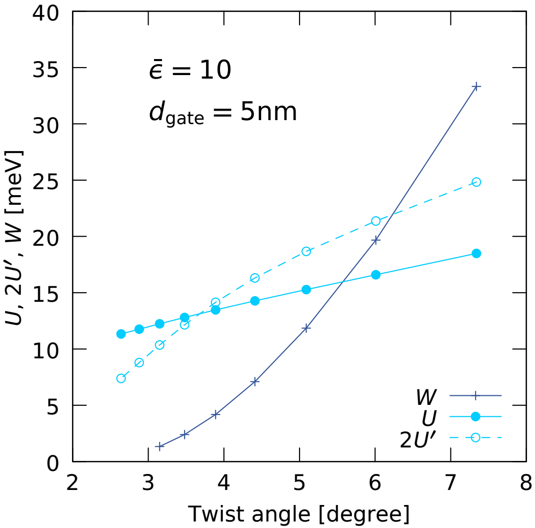

Summary

arXiv:2206.14835

- monolayer BC_3: 3 valley system
- twisted bilayer BC_3: valley dependent quasi-1D bands
  - valleytronics
  - unique model in strongly correlated limit

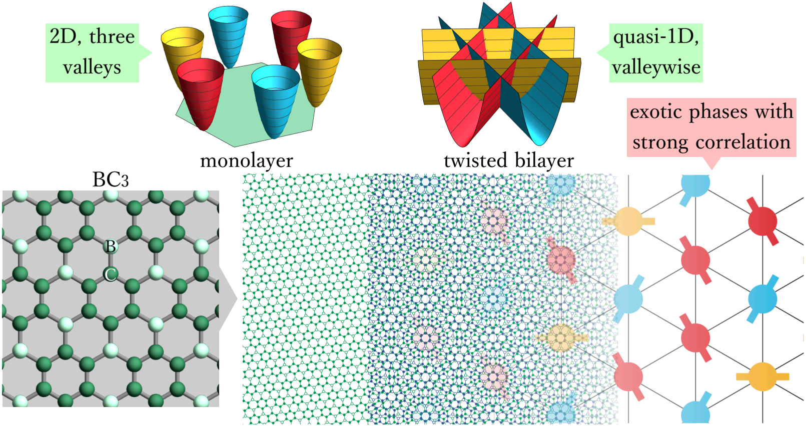

Materials: BC_3 and C_3N

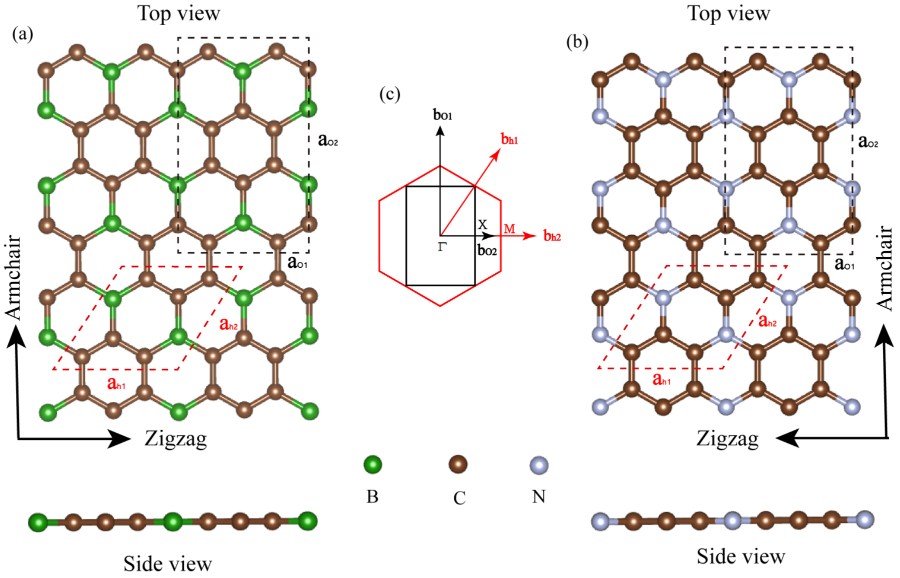

H. Wang *et al.*, J. Appl. Phys. **126**, 234302 (2019).

Experiment: BC_3

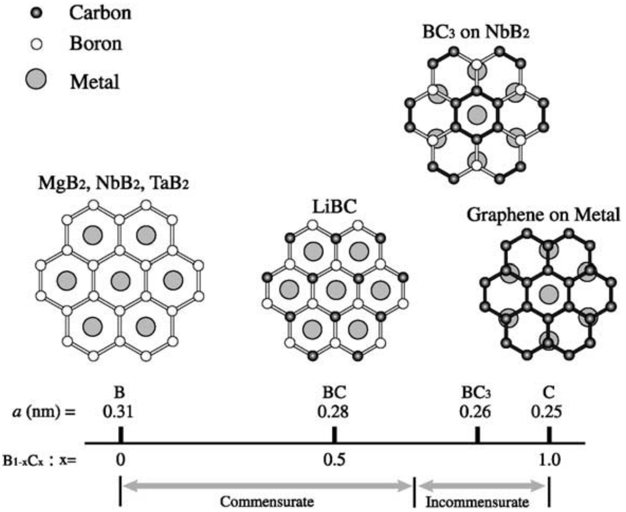

H. Tanaka *et al.*, Solid State Commun. **136**, 22 (2005).

Experiment: BC_3

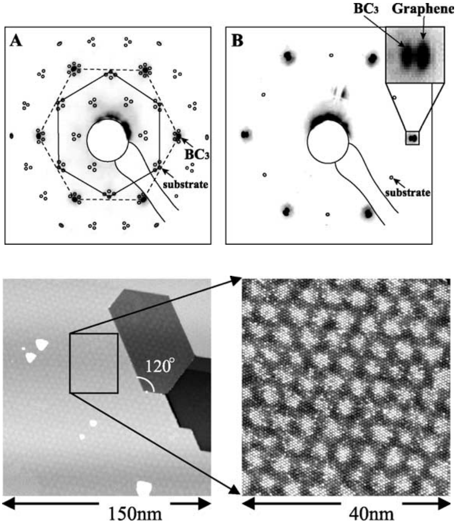

H. Tanaka *et al.*, Solid State Commun. **136**, 22 (2005).

Effective Tunneling and Layer Degeneracy Lifting

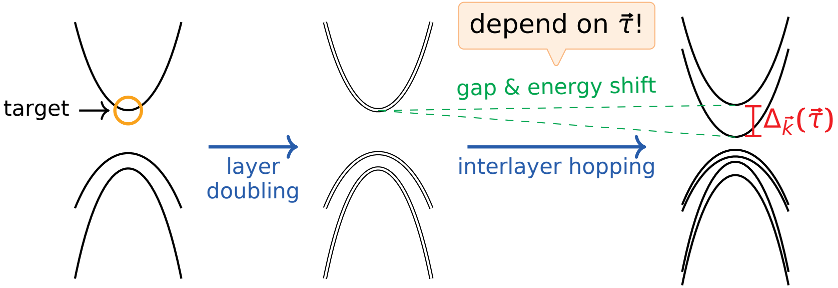

$$\Delta_{\vec{k}}(\vec{\tau}) = |V_{\vec{k}}(\vec{\tau})|, \quad V(\vec{r}) = V_{\vec{k}}(\vec{\tau}(\vec{r}))$$

Degeneracy Lifting